Compact Low Profile UHF Switched-Beam Antenna for Advanced Tyre Monitoring Systems

Gregor Lasser* Lukas W. Mayer† Christoph F. Mecklenbräuker*

Abstract — **Advanced tyre monitoring systems are based on small sensor units directly embedded into the tyre rubber. In contrast to conventional tyre monitoring systems, more data like vibration information and slip angle are collected at this exposed position, so vehicular safety systems can be further improved. Powering of and communication with these sensor units, could be done with UHF radio frequency identification technology. In this contribution we propose a novel compact switched-beam antenna suitable for UHF frequencies. When mounted below the body floor pan of a vehicle, its directivity of 6 dB and the possibility to switch the main beam direction in 90° steps enables selection of a specific tyre for communication. Finally, we present measurements of the assembled antenna performed in an anechoic chamber.**

1 Introduction

Tyre Pressure Monitoring Systems (TPMS) are categorised in direct systems, which employ sensor units usually mounted at the rim to directly measure the tyre pressure, and indirect systems, which use existing data like wheel rotation to infer from these data on the inflation of the tyres. Only the first category of TPMS enables absolute pressure measurements and enhancements like Advanced Tyre Monitoring Systems (ATMS) [1], which further increase vehicular safety and comfort by providing additional sensor data like slip angle or tyre type and age. Today, conventional direct TPMS mostly operate in the 415 MHz range. For ATMS UHF Radio Frequency Identification (RFID) is considered as a solution for data transfer and power supply. However, due to the lossy nature of tyre rubber layers [2] the radio channel losses are high [3] and read probabilities depend on the antenna orientation in the tyre [4]. To overcome the high channel losses, either the distance between the sensor node antenna and the onboard unit antenna has to be reduced by using separate antennas for each wheelhouse, or a centralised high gain antenna whose beam points at the wheels can be used. In this paper we present a switched-beam antenna, designed to operate at the European and American UHF RFID bands. When mounted below a car body floor pan its switched main beam points at one of the four wheels. This provides higher field strength at the wheel sensor which is selected for communication, while at the same time the field strengths at the other wheels is reduced. This approach has several benefits: Due to the antenna directivity, a part of the large channel losses present in RFID TPMS systems is compensated for a selected wheel. Therefore, the power requirements of the RFID based wheel sensor can be relaxed. When properly adjusted, the transmit signal will only be sufficient to power the sensor in the wheel that is currently selected by the antenna beam. This eliminates the need to identify the wheel sensor by an identification code, which has to be stored to the vehicular electronics manually in current systems. Therefore, when changing tyres the vehicle will automatically learn which sensor is in which wheel. Many switched-beam antennas can be found in literature, however most literature entries deal with phased arrays which are large antenna structures with respect to the wavelength, exceptions being [5–7].

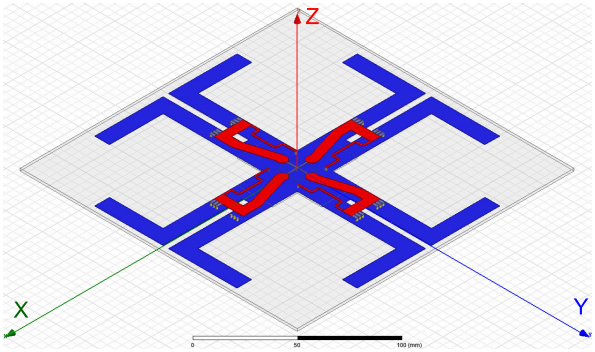

Figure 1: Antenna geometry for simulation showing feeding structure in red.

2 Antenna Principle

The proposed design is based on four dipoles arranged in a geometry similar to a Jerusalem cross, as shown in Fig. 1. The antenna is constructed as a two-layer printed circuit on a 1.5 mm thick fiberglass reinforced substrate of dimensions 0.55 by 0.55 wavelengths. The bottom side of the printed circuit board (PCB) contains the four dipoles which are each connected by a balanced line that leads to

*Vienna University of Technology, Institute of Telecommunications. email: gregor.lasser@tuwien.ac.at
†www.lwm-research.at.
email: lukasw.mayer@lwm-research.at

the antenna centre and terminates in a short circuit. These balanced lines form the plus-shaped part of the Jerusalem cross.

When selecting a specific beam, only one dipole element is fed, and the neighbouring cross arms act as passive reflectors. The top side of the PCB incorporates the feeding network, consisting of two quarter-wavelength lines per element, which are shown red in Fig. 1. A detailed representation of the feeding network including discrete components is given in Fig. 2. A low impedance microstrip line feeds each dipole. Blocking capacitors C1F-C4F and C1A-C4C disconnect the DC current pathes used to control the beam-switching. A second line brings the control signal to the respective switching diodes. These quarter-wavelength biasing lines are short-circuited for RF-signals with the capacitoars C1DC-C4DC. Beam switching is done by means of three parallel PIN-diodes D1A-D4C located at the end of the quarter-wavelength feed lines. Three diodes were connected in parallel to reduce the series inductance of the shorting path. When selecting one beam the respective dipole element is activated by reverse biasing the corresponding PIN-diodes. The three other elements are deactivated by conducting diodes. The quarter-wave feedlines of the deactivated arms thus present a high impedance to the antenna centre where the coaxial cable is attached by an SMA connector. In contrast, the feed line of the active element transforms the impedance at the dipole feedpoint into 50 Ω at the antenna centre. This provides that the power is directed only into the active dipole element.

Fig. 3 presents simulation results in Ansoft's HFSS field simulator. The surface current density is plotted over the back side of the antenna, where currents induced by the feeding network do not appear. The top dipole element is radiating, while the other elements are short-circuited with their corresponding pin diodes. Red areas indicate high current densities, while blue areas indicate low densities. Besides the radiating dipole itself and its corresponding parallel balancing line, there are also noticable currents on the balancing lines of the two dipoles which are oriented orthogonal to the radiating element. These lines and especially the slots of the unused orthogonal dipole balancing lines act as parasitic elements for the radiating dipole and contribute to the directivity of the antenna.

An additional cross shaped PCB in the centre of the antenna depicted in the image of the manufactured antenna in Fig. 4. performs the level conversion from logic control signals to PIN-diode currents. Due to its position at the center of the antenna where surface currents are low, this additional PCB does not affect the antenna parameters.

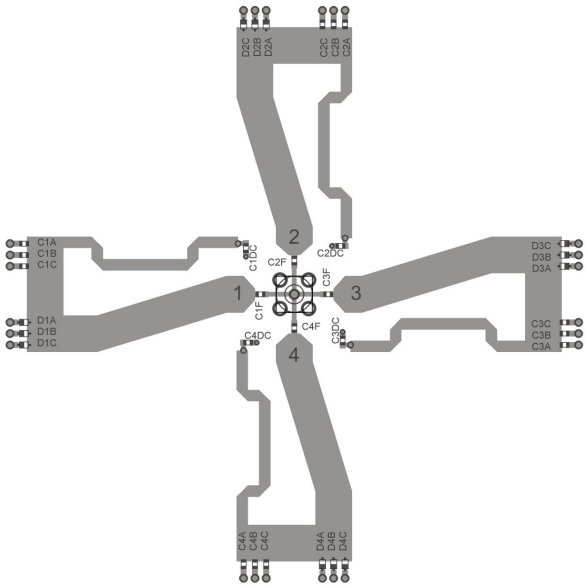

Figure 2: Feeding network including discrete components.

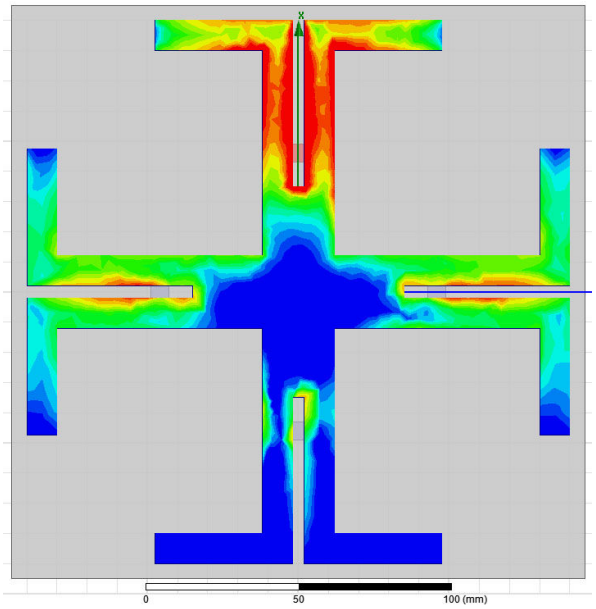

Figure 3: Simulated surface currents on bottom side of the dipole layer at 866 MHz.

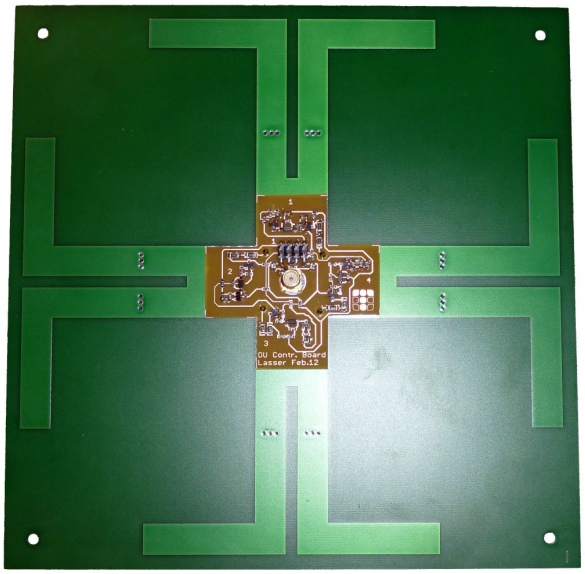

Figure 4: Picture of the manufactured antenna showing radiating elements and PIN-diode control circuitry.

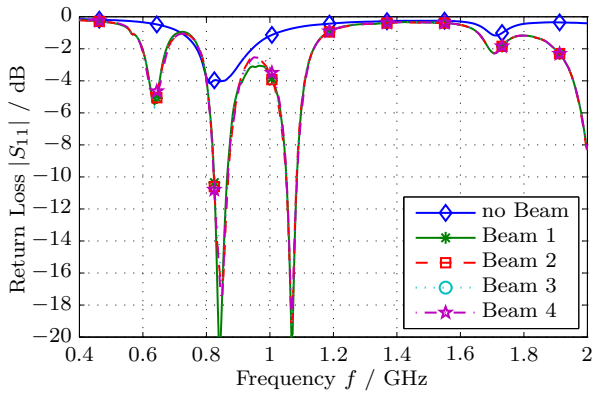

Figure 5: Antenna return loss for different PIN-diode settings.

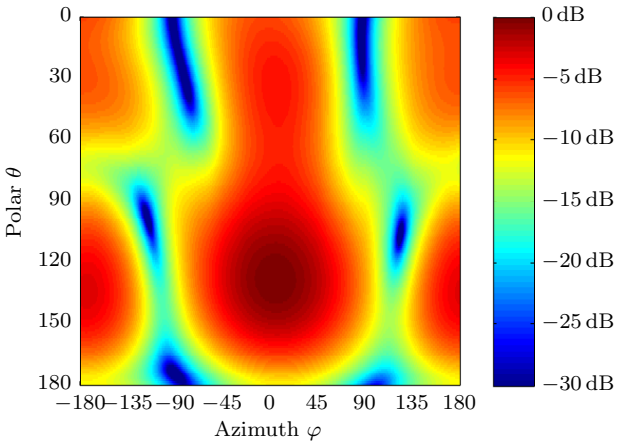

Figure 6: Gain pattern of the antenna switched to beam 1 at 865 MHz for horizontal polarisation, shown as logarithmically scaled pseudo-color plot.

3 Measurement Results

3.1 Return Loss

After assembly of the antenna, the return loss was measured using a vector network analyser. The current through a single PIN-diode was chosen to be 6.4 mA, in the non conducting state the diodes are reverse biased by 12 V. Fig. 5 shows the results of the return loss of the antenna for all four beam settings and for the case when no beam is selected. It can be seen that the four beams behave very similar, which is of no surprise due to the symmetric design of the antenna. When no beam is selected, all diodes are forward biased and thus resemble short-circuits, which are transformed into a high impedance state at the central feed point by the quarter-wavelengths transformers. Consequently, the return loss is low. The losses of the diodes and some parasitic radiation of the quarter-wave feed lines cause a return loss of some 4 dB. The 10 dB bandwidth of the antenna ranges from 824 MHz to 868 MHz which is lower than the original design values. This shift in frequency and slight reduction in bandwidth is most likely caused by the circuit board material (fiberglass reinforced substrate — FR-4) with happens to have a higher permittivity than was assumed in simulations.

To evaluate the influence of possible non-linear behaviour of the PIN-diodes on the return loss, a powersweep ranging from −7 dBm to 33 dBm was performed. The measured variation of the return loss is much smaller than the linearity of the network analyser which is specified with ±0.1 dB.

3.2 Radiation pattern measurements

The antenna was placed in an anechoic chamber and near-field antenna measurements were performed for all four beam settings. The directivity of the antenna was measured to be $D = 6$ dB at 865 MHz. A pseudo-color plot of the transformed far-field pattern for beam 1 is plotted in Fig. 6. All pattern plots are aligned with respect to the coordinate system shown in Fig. 1, so that the horizontal plane corresponds to the xy-plane, and $\varphi = 0°$ corresponds to a positive x-direction. In simulations the main lobe peak is aligned with the xy-antenna plane at a polar angle of $\theta = 90°$. Measurements show a shift to $\theta = 128°$, which the authors believe is caused by disturbance through the central feeding cable running in negative z direction and which was not part of the simulation model. How-

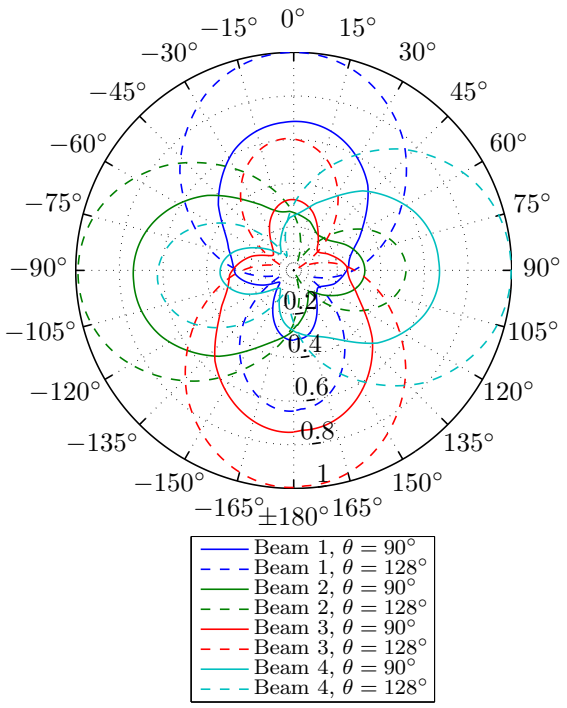

Figure 7: Radiation pattern versus azimuth angle φ at 865 MHz for two polar angles.

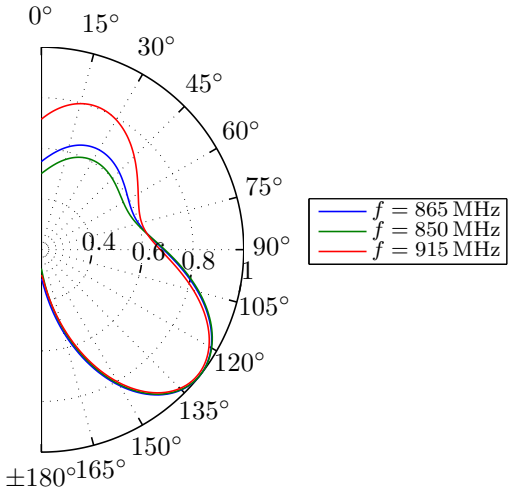

Figure 8: Radiation pattern for beam 1 versus polar angle θ at different frequencies and an azimuth angle $\varphi = 0°$.

ever, the elevation half-power beamwith is above 63° and good coverage is still achieved along the antenna plane.

Fig. 7 shows the radiation far-field pattern of the antenna versus azimuth angle φ. It was plotted for all four beam settings and for two polar angles of $\theta = 90°$ and $\theta = 128°$, where the first angle is represented by solid lines. It is evident from the plot that the individual beams can be steered to the azimuth positions 0°, 90°, 180° and 270°.

Fig. 8 shows the radiation pattern versus polar angle for beam 1 at different frequencies. Towards higher frequencies, a sidelobe with a low polar angle of $\theta = 20°$ becomes stronger.

4 Conclusion

In this contribution a switched-beam antenna for UHF RFID is presented. The proposed antenna is of compact size (0.55 by 0.55 wavelengths) and is constructed as a printed circuit board. PIN-diodes enable switching of the beam in 90° azimuth steps. Measurements show a directivity of 6 dB and an impedance bandwidth of 44 MHz. The proposed antenna provides an efficient way to communicate with RFID tags that are arranged around the antenna. When the power levels are properly adjusted, only tags in the located within the selected beam will communicate with the RFID reader that is connected to the proposed antenna. While this is very useful for many RFID scenarios, it is especially suitable for RFID based vehicular sensor applications like ATMS, because communication with sensors only in the selected wheel is established without knowing sensor IDs.

References

[1] S. C. Ergen, A. Sangiovanni-Vincentelli, X. Sun, R. Tebano, S. Alalusi, G. Audisio, and M. Sabatini, "The tire as an intelligent sensor," *IEEE Trans. Comput.-Aided Design Integr. Circuits Syst.*, vol. 28, pp. 941–955, Jul. 2009.

[2] J. Grosinger, L. W. Mayer, C. F. Mecklenbräuker, and A. L. Scholtz, "Determining the dielectric properties of a car tire for an advanced tire monitoring system," *Vehicular Technology Conference. VTC 2009-Fall. IEEE 70th*, Sep. 2009.

[3] G. Lasser and C. F. Mecklenbräuker, "Dual-band channel measurements for an advanced tyre monitoring system," *Vehicular Technology Conference. VTC 2010-Spring. IEEE 71th*, pp. 1–5, May 2010.

[4] G. Lasser, R. Langwieser, F. Xaver, and C. F. Mecklenbräuker, "Dual-band channel gain statistics for dual-antenna tyre pressure monitoring RFID tags," in *Proceedings of the 2011 IEEE International Conference on RFID*. Orlando, Fl: IEEE, Apr. 2011, pp. 57–61.

[5] J. Sahaya Kulandai Raj, J. Bonney, P. Herrero, and J. Schoebel, "A reconfigurable antenna for MIMO application," in *Antennas Propagation Conference, 2009. LAPC 2009. Loughborough*, Nov. 2009, pp. 269–272.

[6] V. A. Nguyen and P. S. Ook, "Compact switched and reconfigurable 4-ports beam antenna array for MIMO applications," in *Intelligent Radio for Future Personal Terminals (IMWS-IRFPT), 2011 IEEE MTT-S International Microwave Workshop Series on*, Aug. 2011, pp. 1–3.

[7] J. Sahaya Kulandai Raj, J. Fahlbusch, and J. Schoebel, "A beam switching three layer reconfigurable antenna," in *Microwave Conference (GeMiC), 2012 The 7th German*, Mar. 2012, pp. 1–4.